# Asymptotic normalization coefficients for $^8$B $\rightarrow$ $^7$Be + $p$ from a study of $^8$Li $\rightarrow$ $^7$Li + $n$

L. Trache,[1] A. Azhari,[1] F. Carstoiu,[1,2] H.L. Clark,[1] C.A. Gagliardi,[1] Y.-W. Lui,[1]
A.M. Mukhamedzhanov,[1] X. Tang,[1] N. Timofeyuk,[3] and R.E. Tribble[1]

[1]*Cyclotron Institute, Texas A&M University, College Station, TX 77843-3366, USA*
[2]*Institute of Physics and Nuclear Engineering Horia Hulubei, Bucharest, Romania*
[3]*Department of Physics, University of Surrey, Guildford, Surrey GU2 7XH, England, UK*

(Dated: February 8, 2008)

Asymptotic normalization coefficients (ANCs) for $^8$Li $\rightarrow$ $^7$Li + $n$ have been extracted from the neutron transfer reaction $^{13}$C($^7$Li,$^8$Li)$^{12}$C at 63 MeV. These are related to the ANCs in $^8$B $\rightarrow$ $^7$Be + $p$ using charge symmetry. We extract ANCs for $^8$B that are in very good agreement with those inferred from proton transfer and breakup experiments. We have also separated the contributions from the $p_{1/2}$ and $p_{3/2}$ components in the transfer. We find the astrophysical factor for the $^7$Be($p$,$\gamma$)$^8$B reaction to be $S_{17}(0) = 17.6 \pm 1.7$ eV b. This is the first time that the rate of a direct capture reaction of astrophysical interest has been determined through a measurement of the ANCs in the mirror system.

PACS numbers: 26.20.+f, 25.70.Hi, 26.65.+t, 27.20.+n

arXiv:nucl-ex/0304016v1 21 Apr 2003

Recently the SuperK [1] and SNO [2] collaborations have reported measurements of the solar neutrino flux that provide strong evidence for neutrino oscillations. Both experiments are primarily sensitive to high energy solar neutrinos from the $\beta$ decay of $^8$B, produced in the $^7$Be($p$,$\gamma$)$^8$B reaction. Consequently its reaction rate at solar energies has been the subject of many recent studies using both direct [3, 4, 5, 6] and indirect techniques [7, 8, 9, 10, 11].

Previously, we used ($^7$Be,$^8$B) proton transfer reactions to measure the asymptotic normalization coefficients (ANCs) for the $^8$B $\rightarrow$ $^7$Be + $p$ process, from which we determined the astrophysical factor $S_{17}(0)$ [8]. However, in those measurements, the separate contributions of the $p_{1/2}$ and $p_{3/2}$ orbitals could not be inferred from the ($^7$Be,$^8$B) angular distributions. Thus, we used microscopic calculations [12] to fix their relative strengths.

Here we report a study of the mirror neutron transfer reaction, ($^7$Li,$^8$Li), at an energy similar to those used in the proton transfer reactions. $^8$B and $^8$Li are mirror nuclei, and charge symmetry implies that the spectroscopic amplitudes for the proton single particle orbitals entering the $^8$B wave function are nearly the same as those of the neutron single particle orbitals in $^8$Li. Indeed, this has been verified by many theoretical calculations for $^8$Li and $^8$B using a variety of potential models. Calculations have been done using multi-particle shell models [13, 14, 15, 16, 17], microscopic cluster models [18, 19, 20], or a three-body cluster model with long-range correlations [21] with different effective interactions. The absolute values that they predict for the spectroscopic amplitudes differ. However, all calculations agree that spectroscopic factors for the two nuclei are very similar, with differences being smaller than 2-3%. Moreover it was shown in Ref. [22] that microscopic calculations of ANCs for these mirror nuclei are very sensitive to the adopted $NN$ potentials, but their ratio is very stable.

Previously we have shown [23] that the $^8$B overlap function calculated in a single-particle approach is an excellent approximation to that obtained from microscopic calculations. Indeed we have used this fact to obtain ANCs for $^8$B $\rightarrow$ $^7$Be + $p$ from transfer reactions [8]. In this single-particle approach, the spectroscopic factor is related to the ANC by $C^2 = Sb^2$ [24] where $b$ is the single-particle ANC. Thus the mirror symmetry between the spectroscopic factors, coupled with the single-particle approximation, leads to a proportionality between the asymptotic normalization coefficients in $^8$B $\rightarrow$ $^7$Be + $p$ and $^8$Li $\rightarrow$ $^7$Li + $n$ (see Eq. (2)).

Mirror symmetry has been used frequently to obtain spectroscopic information pertinent to astrophysics [25, 26, 27], but its application to direct capture reactions requires care. Although charge-symmetry breaking effects on the spectroscopic amplitudes only arise at the few percent level, this does not provide any relationship between the $^7$Be($p$,$\gamma$)$^8$B proton capture rate and its mirror reaction $^7$Li($n$,$\gamma$)$^8$Li. These reactions proceed via $s$-wave capture at low energies. Proton captures on $^7$Be occur only at large separation distances due to the Coulomb barrier, so their rate at astrophysical energies can be calculated from knowledge of the amplitude of the tail of the $^8$B two-body overlap function in the $^7$Be + $p$ channel, *i.e.* the ANC. In contrast, the absence of any Coulomb barrier coupled with the dominant $s$-wave capture in the $^7$Li + $n$ system implies that the amplitude for the mirror neutron capture reaction may have a substantial contribution from the nuclear interior, and it can not be calculated from the ANC alone. Thus, the proportionality between the ANCs in $^8$B $\rightarrow$ $^7$Be + $p$ and $^8$Li $\rightarrow$ $^7$Li + $n$ does not carry over to the direct capture rates.

We have used the neutron transfer reaction $^{13}$C($^7$Li,$^8$Li)$^{12}$C to obtain the ANCs for $^8$Li $\rightarrow$ $^7$Li + $n$. The use of a stable beam in this experiment allows the measurement of the angular distribution with sufficient resolution that we are able to determine the strengths of the $p_{3/2}$ and $p_{1/2}$ components separately.

Invoking mirror symmetry, we infer the ANCs for $^8$B $\rightarrow$ $^7$Be + $p$ and use them to determine the astrophysical factor $S_{17}$. This is a new variation of the ANC approach that will also be useful in other nuclear systems.

The $^{13}$C($^7$Li,$^8$Li)$^{12}$C neutron transfer reaction at 9 MeV/u is dominated by a direct one-step process in which the last neutron in the target is picked up by the projectile. The process can be well described in DWBA [28] and, as we show below, the transfer is peripheral at this energy. In previous publications [24], we have given a general expression for peripheral reactions relating the angular distribution to DWBA cross sections and the appropriate ANCs. We chose $^{13}$C as a target because it has a relatively loosely bound neutron in a $1p_{1/2}$ orbital around a tightly bound core and the $^{13}$C $\rightarrow$ $^{12}$C + $n$ ANC is known. The differential cross section for the $^{13}$C($^7$Li,$^8$Li)$^{12}$C neutron transfer reaction can be written as

$$\frac{d\sigma}{d\Omega} = S_{p_{1/2}}(^{13}C)\left[S_{p_{3/2}}(^8Li)\sigma^{DW}_{\frac{1}{2},\frac{3}{2}} + S_{p_{1/2}}(^8Li)\sigma^{DW}_{\frac{1}{2},\frac{1}{2}}\right]$$
$$= \frac{(C^{^{13}C}_{^{12}C,\frac{1}{2}})^2}{b^2_{^{12}C,\frac{1}{2}}}\left[\frac{(C^{^8Li}_{^7Li,\frac{3}{2}})^2}{b^2_{^7Li,\frac{3}{2}}}\sigma^{DW}_{\frac{1}{2},\frac{3}{2}} + \frac{(C^{^8Li}_{^7Li,\frac{1}{2}})^2}{b^2_{^7Li,\frac{1}{2}}}\sigma^{DW}_{\frac{1}{2},\frac{1}{2}}\right], \quad (1)$$

where $\sigma^{DW}_{\frac{1}{2},\frac{3}{2}}$ and $\sigma^{DW}_{\frac{1}{2},\frac{1}{2}}$ are the DWBA cross sections for the $p_{1/2} \rightarrow p_{3/2}$ and $p_{1/2} \rightarrow p_{1/2}$ transitions. $S_j(X)$ are the spectroscopic factors in nucleus $X$, $C^X_{Y,j}$ are the ANCs for $X \rightarrow Y + n$, and $b_{Y,j}$ are the ANCs of the normalized single particle bound state neutron wave functions that are assumed in the DWBA calculations. For a neutron bound to the core, the Whittaker function appearing in the asymptotic behavior of the radial wave function in the proton case [24] must be replaced by the corresponding Hankel function. In the present case the calculated angular distributions for the two $j$ orbitals differ at small angles, which permits their contributions to be disentangled. To determine the ANCs for $^8$Li $\rightarrow$ $^7$Li + $n$, $(C^{^8Li}_{^7Li,\frac{3}{2}})^2$ and $(C^{^8Li}_{^7Li,\frac{1}{2}})^2$ (denoted below as $C^2_{p_{3/2}}$ and $C^2_{p_{1/2}}$), we need to know the ANC $(C^{^{13}C}_{^{12}C,\frac{1}{2}})^2$. However, the ratio of the ANCs in $^8$Li can be obtained without using $(C^{^{13}C}_{^{12}C,\frac{1}{2}})^2$.

Charge symmetry implies that, to a good approximation, the spectroscopic amplitudes of $^8$Li and $^8$B are the same, as demonstrated by the theoretical calculations discussed above. Consequently, from the relationship $(C^X_{Y,j})^2 = S_j(X)(b^X_{Y,j})^2$ [24], one can relate the ANCs in $^8$B to those in $^8$Li,

$$C^2_{p_j}(^8B) = C^2_{p_j}(^8Li)\ b^2_{p_j}(^8B)/b^2_{p_j}(^8Li). \quad (2)$$

The single particle ANCs differ due to the different binding energies and the effect of the Coulomb interaction on the $^8$B radial wave functions.

The experiment was carried out with a 9 MeV/u beam of $^7$Li$^{+1}$ ions from the K500 superconducting cyclotron at Texas A&M University. The beam was transported through the beam analysis system to the scattering chamber of the MDM magnetic spectrometer, where it interacted with a 300 $\mu$g/cm$^2$ $^{13}$C target. The target thickness was determined off-line using the energy loss of $^{228}$Th and $^{241}$Am $\alpha$ sources and confirmed on-line using the energy loss of the beam. The experimental setup, including the focal plane detector, was identical to that described in Ref. [29]. The acceptance of the MDM spectrometer was limited to 4° in the horizontal by 1° in the vertical. An energy resolution of 120 keV and an angular resolution of 0.18°, both FWHM, were obtained for the $^8$Li reaction products. Data for the transfer reaction were obtained for spectrometer settings between −2° and 32°, which covers 0° to 54° in the center-of-mass frame. The angular range $\Delta\theta_{lab} = 4°$ covered by the entrance slit was divided into eight bins in the analysis, each point integrating over $\delta\theta_{lab} = 0.5°$. Typically we moved the spectrometer by 3° at a time, allowing for an overlap that provided a self-consistency check of the data. The beam current was integrated with a calibrated Faraday cup at angles larger than 4°. For angles around 0°, we moved the spectrometer in 2° steps, and the data were normalized by matching with an overlapping angular region. This bootstrap approach was used for spectrometer settings out to 4°. Measurements with the spectrometer on both sides of 0° were made to check beam alignment. The angular distribution for the population of the $^8$Li ground state is shown in Fig. 1.

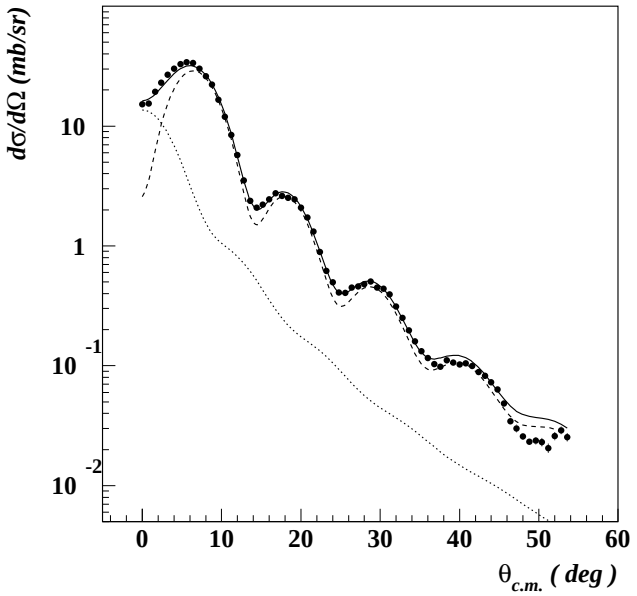


FIG. 1: The angular distribution for the $^{13}$C($^7$Li,$^8$Li)$^{12}$C reaction. The data are shown as points, and the solid line is the best fit. The $p_{1/2} \rightarrow p_{1/2}$ component is shown as a dotted line, and the $p_{1/2} \rightarrow p_{3/2}$ component is the dashed line.

DWBA calculations for the transfer reaction were carried out with the code PTOLEMY [30]. Entrance channel optical model parameters were obtained by fitting $^7$Li + $^{13}$C elastic scattering data at 9 MeV/u with a Woods-

TABLE I: The different optical model parameters used for the DWBA calculations. The entrance/exit channel parameters were obtained from phenomenological fits to $^7$Li+$^{13}$C, $^7$Li+$^{12}$C, and $^6$Li+$^{13}$C elastic scattering angular distributions, and from the double-folding procedure. See text for further explanations.

| Potential | $V$ | $W$ | $r_V$ | $r_W$ | $a_V$ | $a_W$ |
|---|---|---|---|---|---|---|
| | [MeV] | [MeV] | [fm] | [fm] | [fm] | [fm] |
| POT1 | 54.3 | 29.9 | 0.92 | 1.03 | 0.79 | 0.69 |
| POT2 | 99.8 | 22.0 | 1.01 | 0.77 | 0.81 | 0.81 |
| average | 0.366 | 1.00 | | | | |
| fit | 0.323 | 1.00 | | | | |
| $^7$Li+$^{12}$C | 97.8 | 18.8 | 0.79 | 0.97 | 0.71 | 0.95 |
| $^6$Li+$^{13}$C | 77.5 | 16.8 | 0.88 | 1.10 | 0.74 | 0.81 |
| JLM-WS | 58.8 | 21.4 | 0.91 | 1.14 | 0.72 | 0.70 |

Saxon form, as reported in Ref. [29]. The potentials labeled 1 and 2 from Table II of Ref. [29] were used. Calculations were carried out using the same parameters for the exit channel, $^8$Li+$^{12}$C. In addition, calculations were done with entrance/exit channel optical potentials which were obtained from folding-model potentials using the JLM(1) effective interaction [31] following the prescription developed in Ref. [29], and with phenomenological potentials from elastic scattering experiments for similar systems. A summary of the potentials used is presented in Table I. Parameters from Ref. [29] are given in rows 1 through 4. In rows 3 and 4 the renormalization coefficients $N_V$ and $N_W$ of the folded potentials are given instead of the potential depth. We used both the average renormalizations ('average') and those specifically fitted for the $^7$Li+$^{13}$C case at 63 MeV ('fit'). In rows 5 and 6 we list potential parameters extracted from neighboring systems at the same energy per nucleon. The last row (labeled JLM-WS) was obtained by fitting the exit channel folded potentials in the surface region ($r = 3-12$ fm) with Woods-Saxon shapes and renormalizing the depths with the average $N_V$ and $N_W$.

Two components, $p_{1/2} \rightarrow p_{3/2}$ and $p_{1/2} \rightarrow p_{1/2}$, contribute to the $^{13}$C($^7$Li,$^8$Li)$^{12}$C reaction. Results of the DWBA calculations using the POT1 entrance and exit channel potential are shown in Fig. 1. The angular distribution for the $p_{1/2} \rightarrow p_{1/2}$ component has a characteristic $l_{tr} = 0 + 1$ shape, while that for the $p_{1/2} \rightarrow p_{3/2}$ component has a different $l_{tr} = 1 + 2$ shape. The data obtained for center-of-mass angles between 0° and 30° allow for a clear separation of the two components. Larger angles were not used due to increased contributions from multistep processes. Combining the two components leads to the solid line fit.

In order to verify that the transfer reaction is peripheral, calculations with the POT1 potential parameters were carried out using seven different geometries for the Woods-Saxon potential well that binds the last neutron to the $^7$Li core. Both spectroscopic factors and ANCs were extracted for each calculation. Figure 2 shows the

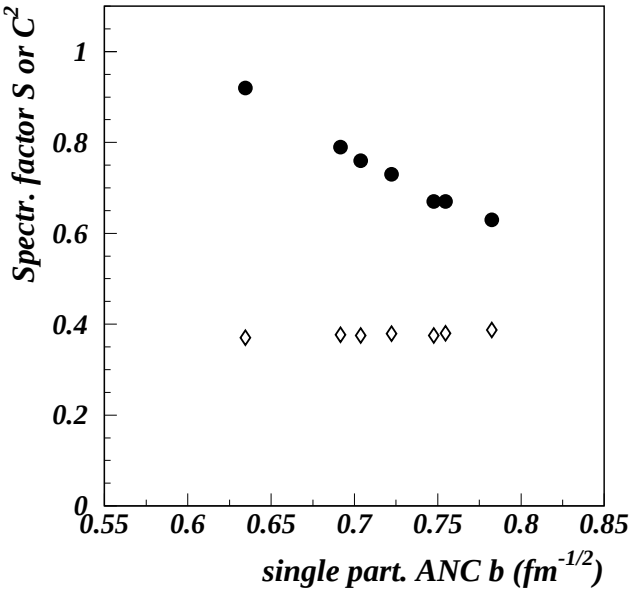


FIG. 2: Comparison of the spectroscopic factors (dots) and of the ANC $C^2$ (diamonds) extracted in the present experiment, for different geometries of the single particle Woods-Saxon well. Only the results for the $p_{3/2}$ component are shown.

TABLE II: The results of the present study for different optical model parameters used for the DWBA calculations. The entrance/exit channel combinations refer to the potentials in Table I. See text for further explanations.

| Potentials | $C^2_{p_{3/2}}$ | $C^2_{p_{1/2}}$ | $\frac{C^2_{p_{1/2}}}{C^2_{p_{3/2}}}$ | $\chi^2$ | angular |
|---|---|---|---|---|---|
| entrance/exit | [fm$^{-1}$] | [fm$^{-1}$] | | | fit range |
| POT1/POT1 | 0.378 | 0.044 | 0.117 | 1.9 | 0-30 deg |
| POT2/POT2 | 0.367 | 0.045 | 0.124 | 5.1 | 0-30 deg |
| POT1/aver | 0.369 | 0.052 | 0.140 | 5.7 | 0-25 deg |
| POT1/aver | 0.379 | 0.052 | 0.139 | 4.8 | 0-20 deg |
| aver/aver | 0.363 | 0.049 | 0.136 | 17.4 | 0-30 deg |
| aver/aver | 0.384 | 0.054 | 0.140 | 5.7 | 0-20 deg |
| fit/aver | 0.390 | 0.053 | 0.136 | 4.6 | 0-20 deg |
| fit/fit | 0.376 | 0.053 | 0.141 | 5.8 | 0-20 deg |
| POT1/$^7$Li+$^{12}$C | 0.370 | 0.044 | 0.118 | 2.5 | 0-30 deg |
| POT1/$^6$Li+$^{13}$C | 0.409 | 0.047 | 0.115 | 2.9 | 0-30 deg |
| POT1/JLM-WS | 0.408 | 0.047 | 0.114 | 3.0 | 0-30 deg |
| w. average | 0.384 | 0.048 | 0.125 | | |

results, plotted against the single particle ANC $b_{sp}$, for the dominant $p_{3/2}$ component. The spectroscopic factors vary ±20% around the average, whereas the ANCs vary less than ±2%, demonstrating that only the asymptotic part of the wave function contributes in the DWBA calculations and the transfer is peripheral. A similar result is found for the $p_{1/2}$ component. The ANCs extracted are therefore independent of the geometry of the single particle potential well used, whereas the spectroscopic factors are not.

Results obtained with different combinations of entrance/exit channel optical potentials are given in Table II. Calculations done with folded potentials used the JLM(1) potentials with the corresponding projectile-target combination at the appropriate energy for each channel and the renormalization values given in Table I. The extracted ANCs are given along with their ratio. We find $C^2_{p_{1/2}}/C^2_{p_{3/2}} = 0.13(2)$. The uncertainty is derived from the standard deviation of the values obtained for different optical potentials and from the uncertainties arising from the angular range used in the fits. This ratio does not depend on the ANC for the ground state of $^{13}$C or on the absolute values of the individual ANCs in $^8$Li, and is measured for the first time here.

To determine the absolute values of the ANCs in $^8$Li, the ANC in $^{13}$C was taken to be $(C^{^{13}C}_{^{12}C,\frac{1}{2}})^2 = 2.35 \pm 0.12$ fm$^{-1}$, as calculated from the value of the nuclear vertex constant, $G^2 = 0.39 \pm 0.02$ fm, reported in [32]. The results given in Table II show small differences which arise, in part, from neglecting a small core-core correction in the nuclear part of the transition operator for the numerical potentials. Differences also arise from the different renormalizations used, from the inability of the Woods-Saxon shapes to reproduce the actual shape of double-folded potentials and from the angular range used in the fits. In particular, the fits with angular distributions calculated using numerical potentials are not good at larger angles and consequently have larger $\chi^2$ values. This is apparent from the $\chi^2$ values shown in Table II for the same calculations fit over different angular ranges. Overall, the results of the calculations are quite consistent. The variations obtained when using different optical potentials were used to estimate the uncertainties from the calculations. Weighing the calculations by $\chi^2$ gives $C^2_{p_{3/2}}(^8Li) = 0.384 \pm 0.038$ fm$^{-1}$ and $C^2_{p_{1/2}}(^8Li) = 0.048 \pm 0.006$ fm$^{-1}$. Other averaging procedures give essentially identical results. The uncertainty in $C^2_{p_{3/2}}$ includes contributions from the overall normalization of the cross section (7%), choice of the angular range of the fit and the optical model potentials (5%), geometry of the neutron binding potential used in the DWBA calculations (1.5%), and the absolute value of the $^{13}$C ANC (5%). For the smaller component, $C^2_{p_{1/2}}$, the uncertainty in the fit due to different optical model potentials (8%) dominates.

The first excited state in $^8$Li, which is the mirror of the resonance at $E_{cm} = 633$ keV in the $^7$Be$(p,\gamma)^8$B reaction, was also measured in the present experiment. The angular distribution is shown in Fig. 3, where it is compared with a fit using the POT1 optical model parameters. The same two components, $p_{1/2} \rightarrow p_{3/2}$ and $p_{1/2} \rightarrow p_{1/2}$, were calculated. The results from the fit are $C^2_{p_{3/2}}(^8Li^*) = 0.067 \pm 0.007$ fm$^{-1}$ and $C^2_{p_{1/2}}(^8Li^*) = 0.015 \pm 0.002$ fm$^{-1}$. The ratio of the ANCs is $C^2_{p_{1/2}}/C^2_{p_{3/2}}(^8Li^*) = 0.22(3)$. Reference [21] predicts a ratio of 0.35 for this state.

To obtain the ANCs in $^8$B corresponding to those in $^8$Li, we use Eq. (2) and assign an additional 3% uncertainty to account for possible charge-symmetry breaking effects. The ratio of the proton and neutron single particle ANCs is $b^2_{p_j}(^8B)/b^2_{p_j}(^8Li) = 1.055(20)$. This ratio was obtained from single-particle wave functions calculated numerically for a neutron or a proton bound in a Woods-Saxon potential with the same geometry and the same spin-orbit interaction and with a depth adjusted to reproduce the experimental neutron or proton binding energy in $^8$Li or $^8$B. The potential depths were found to be nearly equal as the geometrical parameters were varied. This result is the same for both spin-orbit partners and the small uncertainty represents the weak dependence on the geometry of the potential that binds the proton or neutron around its respective core. Inserting this ratio into Eq. (2), we find $C^2_{p_{3/2}}(^8B) = 0.405 \pm 0.041$ fm$^{-1}$ and $C^2_{p_{1/2}}(^8B) = 0.050 \pm 0.006$ fm$^{-1}$. The use of the experimental determination of ANCs in $^8$Li to obtain those in $^8$B was suggested in Ref. [22] based on results of microscopic calculations for the two nuclei, but the ratios found there are somewhat different from the present one and their spread is considerably larger. However, in Ref. [22] the ratio is exaggerated because exactly the same model wave functions were used for the mirror nuclei $^8$B and $^8$Li. An evaluation within a single-particle model shows that the replacement of the neutron bound state wave function in the source term by the proton wave function leads to a decrease of the ratio by 9%, bringing the result of Ref. [22] into agreement with the number above.

The values found for the $^8$B ANCs are in good agreement with those obtained from proton transfer reactions at 12 MeV/u [8], where the average of the values extracted in two similar experiments on different targets

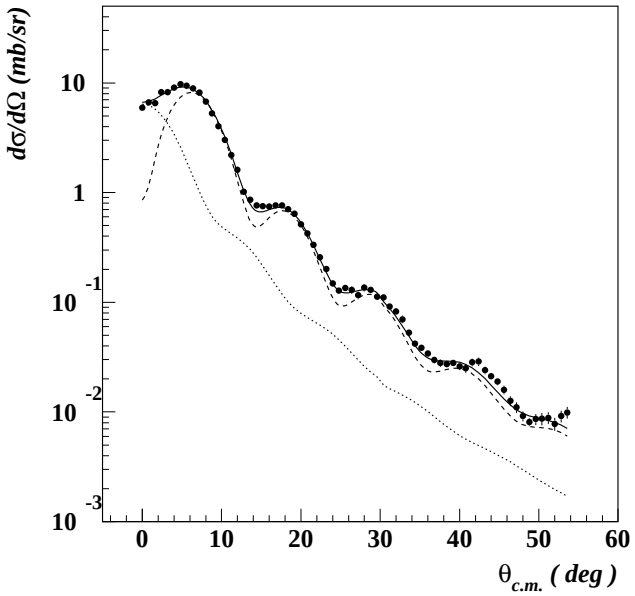


FIG. 3: Same as Fig. 1, but for the first excited state in $^8$Li at 981 keV.

was found to be $C^2_{p_{3/2}}(^8B) = 0.388 \pm 0.039$ fm$^{-1}$. The two spin-orbit components could not be separated there, so the value of 0.157 for the ratio, as predicted from a microscopic model calculation [12], was used to extract the ANCs from the ($^7$Be,$^8$B) reactions. Changing this ratio to 0.13 decreases the value of $S_{17}(0)$ extracted from the proton transfer reactions by only 0.7%.

In Ref. [10] the sum of the ANCs in $^8$B was extracted from breakup reactions at intermediate energies. The value found was $C^2_{p_{3/2}} + C^2_{p_{1/2}} = 0.450 \pm 0.039$ fm$^{-1}$. The present result gives $C^2_{p_{3/2}} + C^2_{p_{1/2}} = 0.455 \pm 0.047$ fm$^{-1}$, in excellent agreement with the value from breakup. Thus the two different transfer reactions and $^8$B breakup all give similar values for the astrophysical factor, the present data giving $S_{17}(0) = 17.6 \pm 1.7$ eV b. This result is also in agreement, within uncertainties, with most of the existing results for $S_{17}(0)$ from direct or indirect methods [3, 4, 7, 9]. It is not in good agreement with the two latest results from direct measurements [5, 6], which claim very good accuracy. However, the present result is in good agreement with a very recent, high precision Coulomb dissociation study [11] that also calls into question the low-energy extrapolation [33] adopted by the recent direct measurements. In fact, the value of $S_{17}(0)$ inferred from the measurements in Ref. [6] also agrees with our result when the extrapolation to zero energy is done using the prescription in Ref. [11], rather than that in Ref. [33].

This is the first time that the rate of a direct capture reaction of astrophysical interest has been determined through a measurement of the ANCs in the mirror nuclear system. This represents a new variation of the asymptotic normalization coefficient technique that will be applicable in the future to other direct radiative transitions of astrophysical interest for which the proton capture ANC can be shown to be proportional to that in the mirror system and which would otherwise only be accessible through experiments with radioactive beams.

One of us (FC) acknowledges the support of the Cyclotron Institute, Texas A&M University, during which part of this work was completed. This work was supported in part by the U. S. Department of Energy under Grant No. DE-FG03-93ER40773, the U. S. National Science Foundation under Grant No. PHY-0140343, the Robert A. Welch Foundation, and EPSRC grant GR/M/82141.

[1] Super-Kamiokande Collaboration, S. Fukuda *et al.*, Phys. Rev. Lett. **86**, 5651 (2001).
[2] SNO Collaboration, Q. R. Ahmad *et al.*, Phys. Rev. Lett. **87**, 071301 (2001); **89**, 011301 (2002).
[3] F. Hammache *et al.*, Phys. Rev. Lett. **86**, 3985 (2001).
[4] F. Strieder *et al.*, Nucl. Phys. **A696**, 219 (2001).
[5] A.R. Junghans *et al.*, Phys. Rev. Lett. **88**, 041101 (2002).
[6] L.T. Baby *et al.*, Phys. Rev. Lett. **90**, 022501 (2003).
[7] N. Iwasa *et al.*, Phys. Rev. Lett. **83**, 2910 (1999).
[8] A. Azhari, V. Burjan, F. Carstoiu, C.A. Gagliardi, V. Kroha, A.M. Mukhamedzhanov, F. M. Nunes, X. Tang, L. Trache, and R.E. Tribble, Phys. Rev. C **63**, 055803 (2001).
[9] B. Davids, S.M. Austin, D. Bazin, H. Esbensen, B.M. Sherrill, I.J. Thompson, and J.A. Tostevin Phys. Rev. C **63**, 065806 (2001).
[10] L. Trache, F. Carstoiu, C.A. Gagliardi and R.E. Tribble, Phys. Rev. Lett. **87**, 271102 (2001).
[11] F. Schumann *et al.*, nucl-ex/0304011.
[12] A.M. Mukhamedzhanov and N. Timofeyuk, Yad. Fiz. **51**, 679 (1990) (Soviet J. Nucl. Phys. **51**, 431 (1990)).
[13] A.M. Khan, Prog. Theor. Phys. **60**, 220 (1978).
[14] B.A. Brown, A. Csoto and R. Sherr, Nucl. Phys. **A597**, 66 (1996).
[15] G. Kim, R.R. Khaydarov, I.-T. Cheon and F.A. Gareev, Nucl. Phys. **A679**, 304 (2001).
[16] K. Bennaceur, F. Nowacki, J. Okolowitz and M. Ploszajczak, Nucl. Phys. **A651**, 289 (1999).
[17] M. Horoi, private communication.
[18] K. Arai, Y. Ogawa, Y. Suzuki and K. Varga, Prog. Theor. Phys. Suppl. **142**, 97 (2001).
[19] A. Csoto, Phys. Lett. **B315**, 24 (1993).
[20] D. Baye, P. Descouvemont and N.K. Timofeyuk, Nucl. Phys. **A577**, 624 (1994); and P. Descouvemont, private communication.
[21] L.V. Grigorenko, B.V. Danilin, V.D. Efros, N.B. Shul'gina and M.V. Zhukov, Phys. Rev. C **60**, 044312 (1999).
[22] N.K. Timofeyuk, Nucl. Phys. **A632**, 19 (1998).
[23] A. M. Mukhamedzhanov, C. A. Gagliardi and R. E. Tribble, Phys. Rev. **C 63**, 024612 (2001).
[24] A.M. Mukhamedzhanov *et al.*, Phys. Rev. C **56**, 1302 (1997).
[25] F.C. Barker, Nucl. Phys. **A588**, 693 (1995).
[26] T. Kajino and G. Mathews, Phys. Rev. C **40**, 525 (1989).
[27] N.K. Timofeyuk and S.B. Igamov, Nucl. Phys. **A713**, 217 (2003).
[28] G.R. Satchler, *Direct Nuclear Reactions*, Clarendon Press, Oxford Univ. Press, N.Y., 1983.
[29] L. Trache, A. Azhari, H.L. Clark, C.A. Gagliardi, Y.-W. Lui, A.M. Mukhamedzhanov, R.E. Tribble and F. Carstoiu, Phys. Rev. C **61**, 024612 (2000).
[30] M. Rhoades-Brown, M. H. Macfarlane, and S. C. Pieper, Phys. Rev. C **21**, 2417 (1980); **21**, 2436 (1980).
[31] J.P. Jeukenne, A. Lejeune and C. Mahaux, Phys. Rev. C **16**, 80 (1977).
[32] N.K. Timofeyuk, D. Baye, and P. Descouvemont, Nucl. Phys. **A620**, 29 (1997).
[33] P. Descouvemont and D. Baye, Nucl. Phys. **A567**, 341 (1994).